Progenitor cell niches in the human pancreatic duct system and associated pancreatic duct glands: an anatomical and immunophenotyping study

Guido Carpino,[1,*] Anastasia Renzi,[2,*] Vincenzo Cardinale,[3] Antonio Franchitto,[2] Paolo Onori,[2] Diletta Overi,[2] Massimo Rossi,[4] Pasquale Bartolomeo Berloco,[4] Domenico Alvaro,[3,†] Lola M. Reid[5,†] and Eugenio Gaudio[2,†]

[1]*Division of Health Sciences, Department of Movement, Human and Health Sciences, University of Rome 'Foro Italico', Rome, Italy*
[2]*Department of Anatomical, Histological, Forensic Medicine and Orthopedics Sciences, Sapienza University of Rome, Rome, Italy*
[3]*Department of Medico-Surgical Sciences and Biotechnologies, Polo Pontino, Sapienza University of Rome, Rome, Italy*
[4]*Department of General Surgery and Organ Transplantation, Sapienza University of Rome, Rome, Italy*
[5]*Department of Cell Biology and Physiology, Program in Molecular Biology and Biotechnology, Lineberger Comprehensive Cancer Center, UNC School of Medicine, Chapel Hill, NC, USA*

Abstract

Pancreatic duct glands (PDGs) are tubule-alveolar glands associated with the pancreatic duct system and can be considered the anatomical counterpart of peribiliary glands (PBGs) found within the biliary tree. Recently, we demonstrated that endodermal precursor niches exist fetally and postnatally and are composed functionally of stem cells and progenitors within PBGs and of committed progenitors within PDGs. Here we have characterized more extensively the anatomy of human PDGs as novel niches containing cells with multiple phenotypes of committed progenitors. Human pancreata ($n = 15$) were obtained from cadaveric adult donors. Specimens were processed for histology, immunohistochemistry and immunofluorescence. PDGs were found in the walls of larger pancreatic ducts (diameters > 300 μm) and constituted nearly 4% of the duct wall area. All of the cells identified were negative for nuclear expression of Oct4, a pluripotency gene, and so are presumably committed progenitors and not stem cells. In the main pancreatic duct and in large interlobular ducts, Sox9^{+} cells represented 5–30% of the cells within PDGs and were located primarily at the bottom of PDGs, whereas rare and scattered Sox9^{+} cells were present within the surface epithelium. The expression of PCNA, a marker of cell proliferation, paralleled the distribution of Sox9 expression. Sox9^{+} PDG cells proved to be Pdx1^{+}/Ngn3^{+/−}/Oct4A^{−}. Nearly 10% of PDG cells were positive for insulin or glucagon. Intercalated ducts contained Sox9^{+}/Pdx1^{+}/Ngn3^{+} cells, a phenotype that is presumptive of committed endocrine progenitors. Some intercalated ducts appeared in continuity with clusters of insulin-positive cells organized in small pancreatic islet-like structures. In summary, PDGs represent niches of a population of Sox9^{+} cells exhibiting a pattern of phenotypic traits implicating a radial axis of maturation from the bottoms of the PDGs to the surface of pancreatic ducts. Our results complete the anatomical background that links biliary and pancreatic tracts and could have important implications for the common patho-physiology of biliary tract and pancreas.

Key words: biliary tract; insulin; pancreas; pancreatic progenitors; stem cell.

Correspondence
Eugenio Gaudio, Department of Human Anatomy, Histology, Forensic Medicine and Orthopedics, Sapienza University of Rome, Via Borelli 50, 00161 Rome, Italy. T/F: + 39 06 49918062; E: eugenio.gaudio@uniroma1.it

*Co-first authors.

†Senior authors.

Introduction

The pancreatic duct system is an intricate network composed of intercalated, intralobular, interlobular and main pancreatic ducts (Udager et al. 2010; Reichert & Rustgi, 2011; Burke & Tosh, 2012). Intercalated ducts are lined by squamous-like epithelial cells and, at the terminal end, by centro-acinar cells interfaced with pancreatic acini. Intralobular and interlobular ducts are lined with cuboidal epithe-

lial cells. Finally, the main pancreatic duct is lined with simple columnar epithelial cells (Reichert & Rustgi, 2011). The main pancreatic duct merges with the common bile duct, forming the hepato-pancreatic common duct opening into the duodenum at the level of the major papilla (Udager et al. 2010; Reichert & Rustgi, 2011; Burke & Tosh, 2012; Cardinale et al. 2012a; Wang et al. 2013).

Liver, biliary tree and pancreas share a common embryological origin (Wandzioch & Zaret, 2009; Udager et al. 2010; Burke & Tosh, 2012; Cardinale et al. 2012a). The embryological development of liver and pancreas in mammals is associated with the appearance of a common endodermal stem/progenitor within the primitive duodenum (Zhou et al. 2007; Wandzioch & Zaret, 2009). This bilio-pancreatic progenitor differentiates in distinct lineages driven by specific transcription factors such as Hes1 in the case of the hepato-biliary fate, or Pdx1/Ngn3/MafA in the case of the pancreatic fate (Reichert & Rustgi, 2011; Kawaguchi, 2013). In particular, Pdx1 is required for specification of all pancreatic lineages, and the expression of Ngn3, MafA, NeuroD, Hnf6, and Pax4 is necessary for endocrine lineage commitment (Reichert & Rustgi, 2011; Kawaguchi, 2013).

Recently, it has been shown that bilio-pancreatic stem/progenitors reside within peribiliary glands (PBGs) in the human biliary tree in fetal and adult tissues (Cardinale et al. 2011; Carpino et al. 2012; Wang et al. 2013). Both intrahepatic and extrahepatic bile ducts contain PBGs within their walls (Cardinale et al. 2011; Carpino et al. 2012; Wang et al. 2013). PBGs contain multiple lineage stages of determined stem/progenitor cell subpopulations [human biliary tree stem/progenitor cells (hBTSCs)] expressing classic endodermal stem cell markers (e.g. Sox2, Nanog, Oct4, Sox9, Sox17, Pdx1) (Cardinale et al. 2011; Carpino et al. 2012, 2014; Semeraro et al. 2012; Wang et al. 2013). Once isolated by immunoselection or culture selection, hBTSCs are able under serum-free, defined conditions to self-replicate for months and then are able to be lineage-restricted under distinct defined conditions into hepatocytes, cholangiocytes or pancreatic islets (Cardinale et al. 2011; Carpino et al. 2012; Wang et al. 2013). Moreover, these hBTSCs were able to correct cirrhosis if injected into the livers of immunocompromised murine hosts (Cardinale et al. 2011; Carpino et al. 2012, 2014; Semeraro et al. 2012) or to correct experimentally induced diabetes if injected into the fat pads of immunocompromised mice treated with streptozotocin (Wang et al. 2013).

Human pancreatic duct glands (PDGs) are glands associated with pancreatic ducts (Strobel et al. 2010); these structures seem to represent the anatomical counterpart of PBGs found within the biliary tree (Nakanuma, 2010). However, the precursor populations isolated from the fetal or adult human pancreata proved to contain only committed progenitors, as indicated by their inability to self-replicate *ex vivo* and by the absence of expression of pluripotency genes (OCT4, SOX2, NANOG, etc.) and other markers typical

of stem cells (Wang et al. 2013). By contrast, those in the fetal and adult biliary tree included both stem cells and committed progenitors (Wang et al. 2013). This interpretation corroborates the findings of others that there are no stem cells, only committed progenitors, in the pancreas postnatally (Zhou et al. 2007; Seifert & Xiong, 2014).

The aims of the present manuscript have been as follows: (1) to study the anatomical distribution of PDGs along the full length of the human pancreatic duct system, (2) to investigate the expression of endodermal progenitor cell and proliferation markers within PDGs, and (3) to describe the spatial distribution of cells expressing endodermal progenitor markers within PDGs and the anatomical organization of PDGs as novel progenitor cell niches.

Materials and methods

Human pancreata ($n = 15$) were obtained from cadaveric donors. All tissues were obtained from the surgical department of Sapienza University of Rome, Italy. Informed consent was obtained from next of kin for use of the tissues for research purposes, the study protocols received Institutional Review Board approval, and processing was compliant with Good Manufacturing Practice. All of the samples were derived from adults, aged 19–73 years, with a median age of 48 (SD 11.89).

Organ donors were routinely screened for underlying pathologies; all specimens included in the present study came from donors without liver (steatosis, viral hepatitis, cirrhosis) or pancreatic (diabetes, pancreatitis) diseases as demonstrated by clinical and serological parameters obtained during transplantation procedures. In accordance, the histological examination of specimens did not show any signs of damage such as inflammation or necrosis.

Pancreas and duodenum were obtained *en bloc* from organ transplantation procedures. The duodenal wall was sectioned, and the major papilla was separated. The head of the pancreas was dissected, and the main pancreatic duct, the common bile duct (choledocus) and the hepato-pancreatic common duct were visualized. For each case, samples were taken (1) at the level of the hepato-pancreatic ampulla, (2) at the level of the main pancreatic duct prior to merging with the choledocus, and (3) at the different levels of the pancreatic body and tail.

Light microscopy (LM), immunohistochemistry (IHC) and immunofluorescence (IF)

Specimens were fixed in 10% buffered formalin for 2–4 h, embedded in low-temperature-fusion paraffin (55–57 °C), and 3- to 4-μm sections were stained with haematoxylin-eosin and Alcian-PAS.

For IHC, sections were mounted on glass slides coated with 0.1% poly-L-lysine. Sections were hydrated in graded alcohol and rinsed in phosphate-buffered saline (PBS, pH 7.4). Endogenous peroxidase activity was blocked by a 30-min incubation in methanolic hydrogen peroxide (2.5%). The endogenous biotin was then blocked by the Biotin Blocking System (code X0590; Dako, Glostrup, Denmark) according to the instructions supplied by the vendor. Antigens were retrieved by applying Proteinase K as suggested by the vendor (code S3020; Dako) for 10 min at room temperature. Sections were then incubated overnight at 4 °C with primary antibodies. A complete list of primary antibodies, sources and dilutions is given in

Table 1. Samples were rinsed twice with PBS for 5 min, and incubated for 20 min at room temperature with secondary biotinylated antibody and then Streptavidin-HRP (both LSAB+ System-HRP, code K0690; Dako). Diaminobenzidine (Dako) was used as substrate, and sections were counterstained with haematoxylin.

For IF, non-specific protein binding was blocked by 5% normal goat serum. Sections were incubated with primary antibodies at room temperature for 1 h. All primary antibodies were diluted in 1% bovine serum albumin in PBS-Tween 20 (PBS-T). The sections were then washed twice with PBS-T and incubated for 1 h with labelled isotype-specific secondary antibodies (dilution 1 : 50): anti-mouse Alexa Fluor-488, -546, anti-rabbit Alexa Fluor-488, -546, anti-goat Alexa Fluor -488, -546, and anti-guinea pig -488 (Alexa Fluor; Invitrogen Ltd, Paisley, UK). They were counterstained with 4′,6-diamidino-2-phenylindole for visualization of cell nuclei. For all immunoreactions, negative controls consisted of the primary antibody being replaced with pre-immune serum.

To perform double IF with two rabbit primary antibodies, we followed a three-step protocol (Nobili et al. 2012): sections were incubated with anti-PDX1 (or anti-NGN3); then, an anti-rabbit secondary fluorescent antibody (AlexaFluor-488) was applied; finally, the antibody for Sox9 was pre-labelled with a fluorophore using the APEX-594 labelling kit (Invitrogen, catalogue #A10474) and was applied to the section. All antibodies were diluted (1 : 50) and incubated at room temperature (RT) for 1 h. Adequate controls were performed (supplementary figures 1–3).

Sections were examined in a coded fashion using the Leica Microsystems DM 4500 B Light and Fluorescence Microscopy (Wetzlar, Germany) equipped with a Jenoptik Prog Res C10 Plus Videocam (Jena, Germany). LM, IHC and IF observations were processed with an Image Analysis System (IAS; Delta Sistemi, Rome, Italy) and were performed independently by two researchers in a blind fashion (Nobili et al. 2014).

Haematoxylin-eosin (H&E) stained slides and IHC stained slides were scanned with a digital scanner (Aperio Scanscope CS System; Aperio Technologies, Inc., Oxford, UK) and processed by ImageScope. For morphometric analysis, the measurement of the duct diameter included the ductal wall; the surface occupied by PDGs was measured as the area occupied by glandular acini (μm^2); and the area fraction with respect to the total area of examined duct wall was also calculated and expressed as a percentage, as done previously (Carpino et al. 2014).

For each organ, three different sections of the main pancreatic duct were separately evaluated at the level of the pancreatic head and of the tail; similarly, up to five interlobular pancreatic ducts were evaluated for each organ; the mean was obtained for each organ and, finally, the data were displayed as mean ± SD of values coming from the 15 organs.

An image analysis algorithm was used to quantify the percentage of cells with Sox9 nuclear expression within PDGs. The number of Sox9^{+} cells was calculated as the percentage of cells with positive nuclei with respect to the total number of cells within PDGs. Counts were performed in all glandular acini in examined ducts.

The number of positive cells for other markers was counted in a random, blinded fashion in six non-overlapping fields (magnification 20×) for each slide. The data are expressed as the percentage of positive cells. Data are summarized by a semi-quantitative score, as done previously: − < 1%; +/− = 1–5%; + = 5–30%; ++ = 30–50%; +++ > 50% (Glaser et al. 2009; Carpino et al. 2012).

Pancreatic ducts were sub-divided into main pancreatic duct, interlobular ducts, intralobular ducts and intercalated ducts according to their anatomical features (Reichert & Rustgi, 2011). For each specimen, at least three different sections of the main pancreatic duct were examined at different levels. At least five different interlobular ducts, intralobular ducts, or intercalated ducts were examined for each specimen.

Many of the markers studied are known to be associated with both stem cells and progenitors; one of the ones expressed by stem cells but not by committed progenitors is nuclear expression of Oct4A, a pluripotency gene (Zhou et al. 2007; Wang et al. 2013; Seifert & Xiong, 2014). Therefore, nuclear, not cytoplasmic, expression of Oct4A was evaluated to identify true stem cells.

Nuclear expression of specific transcription factors, in combination with the findings from our prior studies (Cardinale et al. 2011; Carpino et al. 2012; Wang et al. 2013) and those of others (Zhou et al. 2007; Liu et al. 2014; Seifert & Xiong, 2014) has been interpreted as follows: Oct4A expression recognizes only cells with stem cell phenotype; Sox9, Pdx1, and Lgr5 expression recognize cells with both stem and progenitor cell phenotype; cells with Oct4A^{−}/Sox9^{+}/Pdx1^{+}/Ngn3^{−} phenotype are considered pancreatic committed progenitor cells for both acinar and endocrine fates; Cells with an Oct4A^{−}/Sox9^{+}/Pdx1^{+}/Ngn3^{+} phenotype are considered pancreatic endocrine progenitor cells.

Statistical analysis

Data were expressed as mean ± SEM. Statistical analyses were performed by SPSS statistical software (SPSS Inc., Chicago, IL, USA). Differences between groups for not normally distributed parameters

Table 1 List of antibodies used.

Name	Host/isotype	Source	Catalogue#	Dilution
CK7 (cytokeratin7)	Mouse IgG1	Dako	M7018	1 : 100
Pan-CK	Mouse IgG1	Dako	M7010	1 : 50
Oct4A	Rabbit IgG	Cell Signaling	#2050	1 : 50
Lgr5	Goat IgG	Santa Cruz	SC-68580	1 : 50
PCNA	Mouse IgG2a	Dako	M0879	1 : 100
Pdx1	Rabbit IgG	Santa Cruz	SC-25403	1 : 50
Sox9	Rabbit IgG	Millipore	AB5809	1 : 100
Ngn3	Rabbit IgG	Abcam	Ab38548	1 : 50
	Rabbit IgG	Millipore	AB5684	1 : 200
Glucagon	Rabbit IgG	Santa Cruz	SC-13091	1 : 50
Insulin	Guinea pig IgG	Dako	IS002	1 : 100

were tested by Mann–Whitney U-tests. Statistical significance was set to a P-value < 0.05.

Results

Pancreatic duct gland distribution along human pancreatic duct system

The presence of glandular elements (PDGs) was investigated along the human pancreatic duct system. In accordance with their anatomical division and position, the main pancreatic, interlobular, intralobular and intercalated ducts were studied separately.

The head and the tail of the main pancreatic duct at the head was evaluated. Progressing from the head towards the pancreatic tail, the diameter of the main pancreatic duct decreased progressively from $\approx$ 2000 to $\approx$ 650 μm.

The main pancreatic duct displayed glandular elements located within its wall and called PDGs. PDGs occupied an average area of 50 877 $\pm$ 50 121 μm^2 (Fig. 1). The large variability observed in the areas of the PDGs simply represents the progressive reduction of duct diameter from the pancreatic head to the tail. Therefore, data from main pancreatic duct at the head and at the tail have been considered separately.

Pancreatic duct glands occupied an average area of 104 581 $\pm$ 14 092 μm^2 at the pancreatic head and an average area of 45 166 $\pm$ 6663 μm^2 at the pancreatic tail (P < 0.05); therefore, the PDG area is strictly correlated with the duct diameter (r = 0.69; P < 0.01).

Moreover, the percentage of the duct area (area fraction) occupied by PDGs was 4.11 $\pm$ 1.60% (pancreatic head) and 4.38 $\pm$ 2.63% (pancreatic tail). The PDG area fraction did not correlate with the duct diameter, and no differences
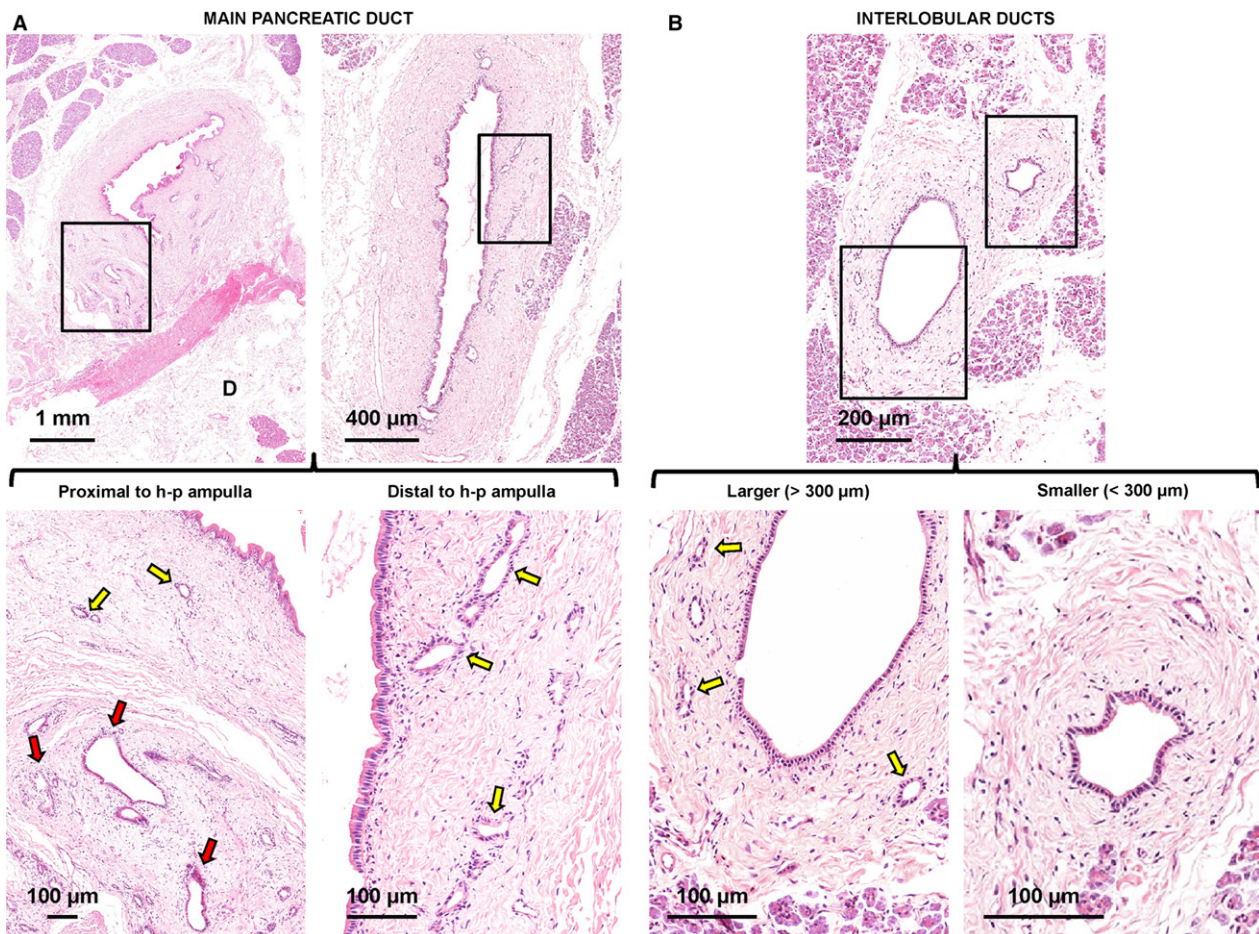

Fig. 1 Distribution of pancreatic duct glands (PDGs) within pancreatic ducts. (A) Haematoxylin-eosin stains of main pancreatic duct. The main pancreatic duct displays glandular elements called PDGs that are located within its wall. The PDG area is strictly correlated with the duct diameter. Near the hepato-pancreatic ampulla, the main pancreatic duct displays two types of glands: intramural (yellow arrows) and extramural (red arrow) PDGs. Distal to the hepato-pancreatic ampulla, only intramural PDGs could be recognized. The area in the boxes is magnified in the lower images. D, duodenum (wall: sub-mucosal layer). (B) Haematoxylin-eosin stain of pancreas. At the level of interlobular pancreatic ducts, PDGs (yellow arrows) are present only in larger ducts (diameter > 300 μm: left images). Smaller interlobular ducts (diameter < 300 μm: right images) do not contain PDGs. Areas in the boxes are magnified in the lower images.

were found when the fraction of the area in the head of the pancreas was compared with that in the pancreatic tail. In the head of the pancreas, but not in the tail, the main pancreatic duct displayed two types of glands: intramural and extramural PDGs. The intramural PDGs were found within the duct wall and appeared as internalized pouches of the surface epithelium, whereas extramural PDGs were located outside and were tethered to the wall of the ducts (Fig. 1A).

The presence of PDGs was investigated at the level of the interlobular pancreatic ducts (IL-PDs). PDGs were present only in larger IL-PDs (diameter > 300 μm). Smaller IL-PDs (diameter < 300 μm) did not have PDGs (Fig. 1B).

Larger IL-PDs had an average diameter = 383.3 ± 22.6 μm; PDGs occupied an average area of 5074 ± 368 μm^2 of the IL-PD wall. This area was lower in comparison with the main pancreatic duct ($P < 0.01$). Moreover, the percentage of the duct area (area fraction) occupied by PDGs was 3.80 ± 2.21%, and was not different in comparison with the main pancreatic duct. Data are summarized in Table 2.

Phenotypic traits cells in pancreatic duct glands

PDGs were partly composed of mucinous acini, which represented 5–30% (semi-quantitative score = +) of glandular cells as demonstrated by both Alcian and PAS positivity (Fig. 2). Mucin-producing cells were more numerous in PDGs associated with the main pancreatic duct than in those associated with interlobular ducts.

The expression of markers representative of endodermal stem and progenitor cells (Oct4A, Sox9, Pdx1, Lgr5, Ngn3) was investigated within PDGs. All PDG cells were negative for Oct4a (data not shown). In the main pancreatic duct and large IL-PDs, [Oct4A$^-$/Sox9$^+$] cells were found within PDGs. In PDGs, these cells represented a sub-population

Table 2 Pancreatic duct gland (PDG) distribution.

	Diameter (μm)	PDG area (μm^2)	PDG volume (%)
Main pancreatic duct (at pancreatic head)	1976.8 ± 183.5*	104 581 ± 14 092*	4.11 ± 1.60
Main pancreatic duct (at pancreatic tail)	1213.4 ± 336.7*	45 166 ± 6663*	4.38 ± 2.63
Large interlobular pancreatic duct	383.3 ± 22.6*	5074 ± 368*	3.80 ± 2.21
Small interlobular pancreatic duct	198.3 ± 61.6*	–	–

Data are expressed as means ± SD.
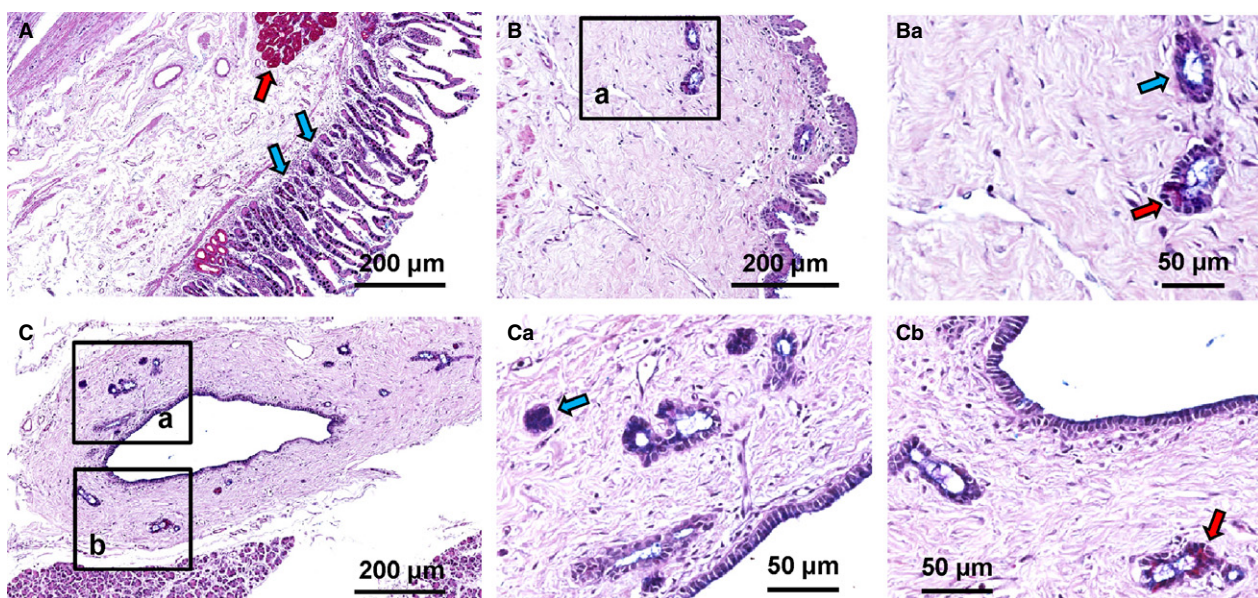*$P < 0.01$ vs. other groups.

Fig. 2 Pancreatic duct glands (PDGs) contain mucin-producing cells. Alcian-PAS (periodic acid Schiff) stain of duodenum (A), main pancreatic duct (B) and interlobular pancreatic ducts (C). (A) In the duodenum, Brunner's glands are PAS-positive (magenta cells: red arrows), whereas goblet cells in intestinal glands are Alcian-positive (purple cells: blue arrows). (B,C) PDGs in main and interlobular pancreatic ducts are PAS$^+$ (red arrows) or Alcian$^+$ (blue arrows). Area in the box in B is magnified in Ba. Areas in the boxes in C are magnified in Ca and Cb.

ranging from 5 to 30% of glandular cells (semi-quantitative score = +) with a mean of 19.5 ± 8.3% (Fig. 3A). No differences were found in the findings from the head vs. the tail of the pancreas. In the main pancreatic duct, Sox9+ cells were located primarily at the bottom of PDGs, whereas rare (less than 5%) and scattered Sox9+ cells were present within the surface epithelium. In the smaller IL-PDs, which lack PDGs, [Oct4A−/Sox9+] cells (semi-quantitative score = ++) were found within the surface epithelium (Fig. 3B).

The expression of PCNA, a marker of cell proliferation, paralleled the distribution of Sox9 (Fig. 3C). PCNA+ cells constituted 17.2 ± 6.5% of cells within PDGs and were not found outside the PDGs. The number of PCNA+ cells decreased progressively in the transitioning to the surface epithelium. At the surface, PCNA+ cells were rare (< 5%).

The percentage of PDG cells positive for Pdx1 [Oct4A−/Sox9+] was 5–30% (semi-quantitative score = +; Fig. 4A). Pdx1 positivity essentially co-localized with Sox9-positivity (Fig. 4B). No differences in Oct4A−/Sox9+/Pdx1+ cell numbers were found in PDGs associated with the main pancreatic duct in the head of the pancreas, with the main pancreatic duct in the pancreatic tail, and in the larger interlobular ducts.

Ngn3+ cells were rare in PDGs associated with the main pancreatic duct (semi-quantitative score = +/−; Fig. 4C, left image), but their percentage increased in PDGs associated with larger interlobular ducts (semi-quantitative score = +; Fig. 4C, right image).

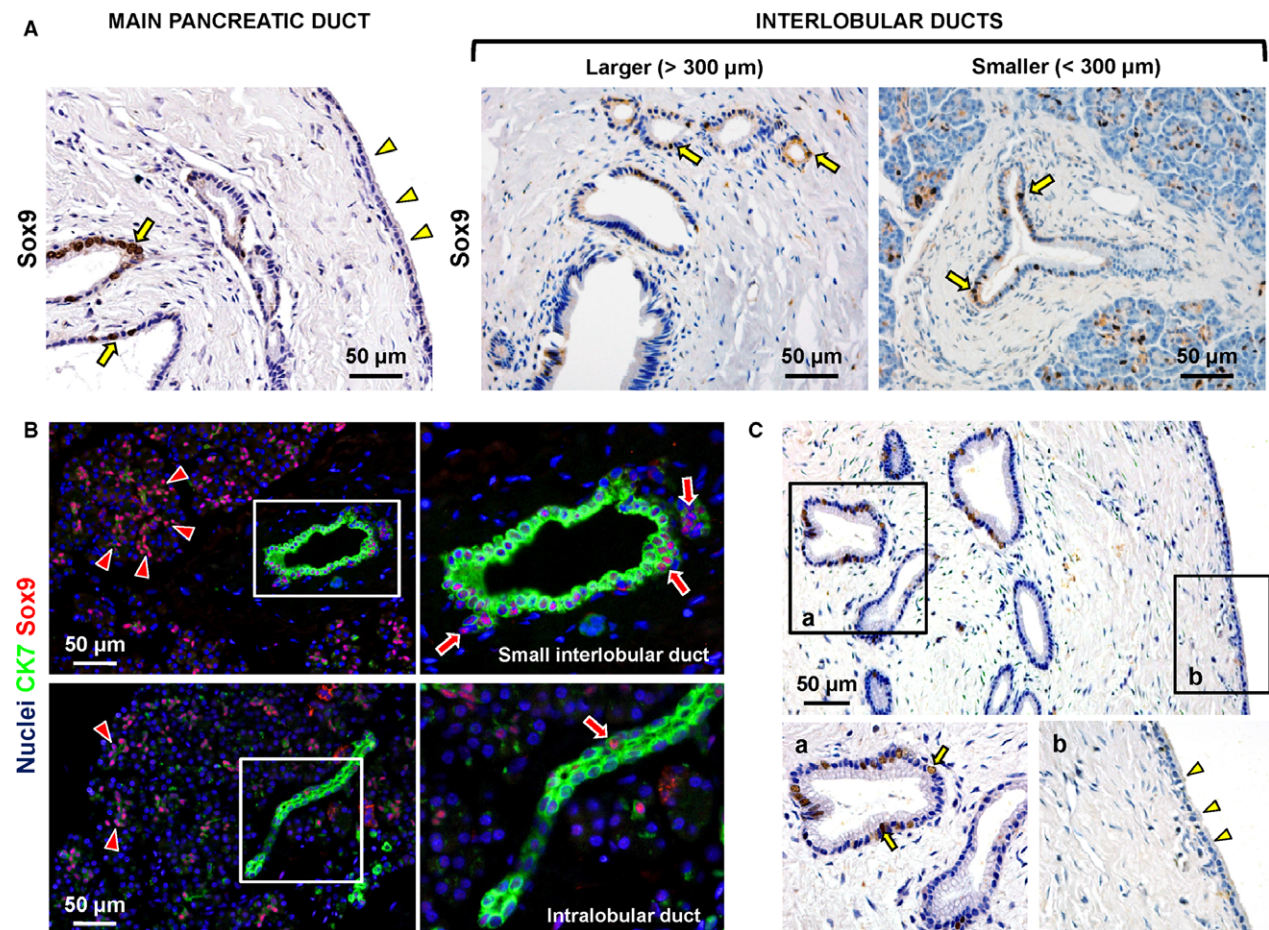Only a few Lgr5+ cells (semi-quantitative score = +/−) were present in PDGs. Lgr5 expression occurred in Sox9+

Fig. 3 Sox9+ cells and proliferating cells are located within pancreatic duct glands (PDGs). (A) Immunohistochemistry for Sox9 in human pancreatic ducts. In the main pancreatic and large interlobular pancreatic ducts, Sox9+ cells (arrows) were evident within PDGs. In PDGs, Sox9+ cells comprise sub-populations ranging from 5 to 30% of glandular cells. In the main and larger interlobular pancreatic ducts, Sox9+ cells were mostly located at the bottom of PDGs (arrows), while rare and scattered Sox9+ cells were present within the surface epithelium (arrowheads). In smaller interlobular pancreatic ducts, Sox9+ cells were found within the surface epithelium (arrows). (B) Double immunofluorescence for CK7 (green) and Sox9 (red). Nuclei are counterstained in blue. Sox9+ cells were present in the small interlobular duct (arrows) and intercalated ducts (arrowheads). A few Sox9+ cells were present in intralobular ducts (lower images, arrow). (C) Immunohistochemistry for PCNA in human pancreatic ducts. The expression of PCNA, a marker of cell proliferation, followed the distribution of Sox9. PCNA+ cells (arrows) were located mostly in PDGs (higher magnification in a). The number of PCNA+ cells progressively decreased with transitions towards the surface epithelium. At the surface (higher magnification in b), epithelial cells were essentially negative for PCNA (arrowheads).
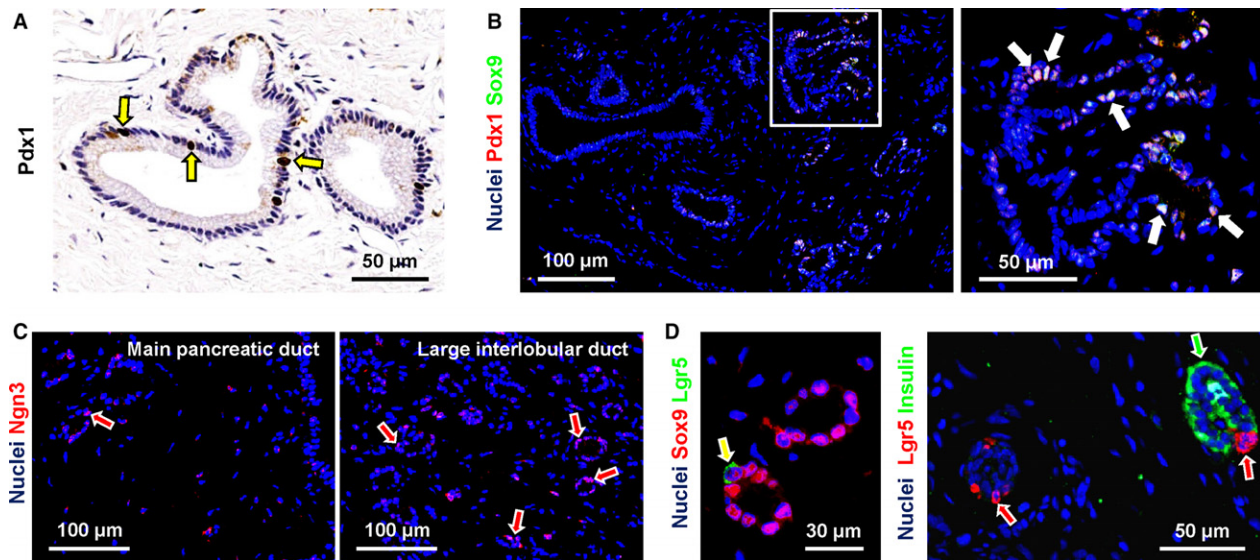
Fig. 4 Expression of progenitor cell markers in pancreatic duct glands (PDGs). (A) Immunohistochemistry for Pdx1 in human pancreas. PDG cells were diffusely positive for Pdx1 (arrows). (B) Double immunofluorescence for Pdx1 (red) and Sox9 (green); the nuclei are displayed in blue. Pdx1 co-localized with Sox9 in the same PDG cells (white nuclei, white arrows). (C) Immunofluorescence for Ngn3. Nuclei are displayed in blue. Ngn3$^+$ cells were more numerous in PDGs associated with large interlobular ducts (arrows in right image) in comparison with the main pancreatic duct (left image). (D) Double immunofluorescence for Lgr5 and Sox9 (left) or insulin (right); the nuclei are displayed in blue. Left image: Lgr5$^+$ cells co-expressed Sox9 (arrow). Right image: Lgr5$^+$ cells (red arrows) were negative for insulin (green arrow).

cells but not in insulin$^+$ ones (Fig. 4D) or glucagon$^+$ ones (data not shown) within PDGs.

The expression of insulin and glucagon was investigated within PDGs. Interestingly, $7.6 \pm 2.4\%$ of PDG cells were positive for insulin (Fig. 5A,B) or glucagon (Fig. 5C,D). Insulin$^+$ (or glucagon$^+$) cells were more numerous in IL-PDs than in the main pancreatic duct ($P < 0.05$).

Phenotypic traits of cells within finer branches of the pancreatic duct system

Beside PDGs, endodermal stem cell and progenitor cell markers (Oct4a, Sox9, Pdx1, Lgr5, Ngn3) were investigated in the finer branches of the pancreatic duct system (i.e. intralobular and intercalated ducts). All were negative for Oct4a (data not shown). Cells within intercalated (semi-quantitative score = +++) but not in intralobular ducts (semi-quantitative score = +/−) were diffusely positive for Sox9 (Fig. 3B). Sox9$^+$ cells in intercalated ducts were also diffusely positive for Pdx1 (semi-quantitative score = +++; Fig. 6A,B) and Ngn3 (semi-quantitative score = ++; Fig. 6C, D). Intercalated ducts were essentially negative for Lgr5 (data not shown). Accordingly, centro-acinar cells (the terminal end duct cells interfacing with acini) were positive for Sox9, Pdx1 and Ngn3 but negative for Lgr5 and Oct4.

Moreover, intercalated ducts were essentially negative for insulin and glucagon (Fig. 6E). Nevertheless, intercalated ducts were observed in direct continuity with clusters of insulin$^+$ cells organized in small pancreatic islet-like structures. In these cases, CK7$^+$ duct cells were in direct continu-

ity with islets. Moreover, CK7$^+$/insulin$^+$ cells were present at the interfaces between ducts and islets (Fig. 6E). Intercalated duct cells in continuity with endocrine islets had Sox9$^+$ nuclei. Moreover, with transitioning from ducts to islets, cells lost nuclear Sox9 positivity (Fig. 6F). Lgr5$^+$ cells were also present (two to three cells per islet) within pancreatic islets, but Lgr5 positivity did not overlap with Sox9 and or with insulin expression (Fig. 6G).

Discussion

The primary findings of the present study are: (1) the PDGs in human pancreas are present only in the walls of larger pancreatic ducts (diameter > 300 μm) and constitute ≈ 4% of the duct wall area, irrespective of the duct size; (2) PDGs represent niches consisting of a heterogeneous population of Sox9$^+$ cells; (3) the phenotypic traits of Sox9$^+$ cells within adult PDGs are consistent with those of pancreatic committed progenitor cells; (4) insulin$^+$ cells are located also within human PDGs but there was no overlap in expression of insulin and various progenitor markers.

A large body of literature supports the currently accepted interpretation that the postnatal pancreas contains committed progenitors, but not stem cells (Zhou et al. 2007; Xu et al. 2008; Strobel et al. 2010; Smukler et al. 2011; Lysy et al. 2012; Seifert & Xiong, 2014; Razavi et al. 2015; Yamaguchi et al. 2015). Although OCT4 and SOX2, classic pluripotency genes, were found in rare cells in the postnatal pancreas, their expression was found to be cytoplasmic, not nuclear (Smukler et al. 2011). Subsequent studies revealed

Fig. 5 Expression of pancreatic endocrine markers in pancreatic duct glands (PDGs). (A) Immunohistochemistry for insulin in human pancreas. PDG cells were positive for insulin (arrow in the right image). Area in the box is magnified in the right image. Insulin⁺ pancreatic islets were present (arrowheads) and represented the positive control. (B) Double immunofluorescence for insulin (green) and cytokeratin7 (CK7: red); the nuclei are displayed in blue. Insulin⁺ cells within PDGs are CK7⁺ (arrow). (C,D) Double immunofluorescence for insulin (green) and glucagon (red); the nuclei are displayed in blue. Glucagon⁺ cells were present within PDGs (magnified in D: arrow). Insulin⁺ and glucagon⁺ pancreatic islet cells were present (magnified in D) and represented positive controls. Acinar cells and intercalated ducts were essentially negative for insulin and glucagon.
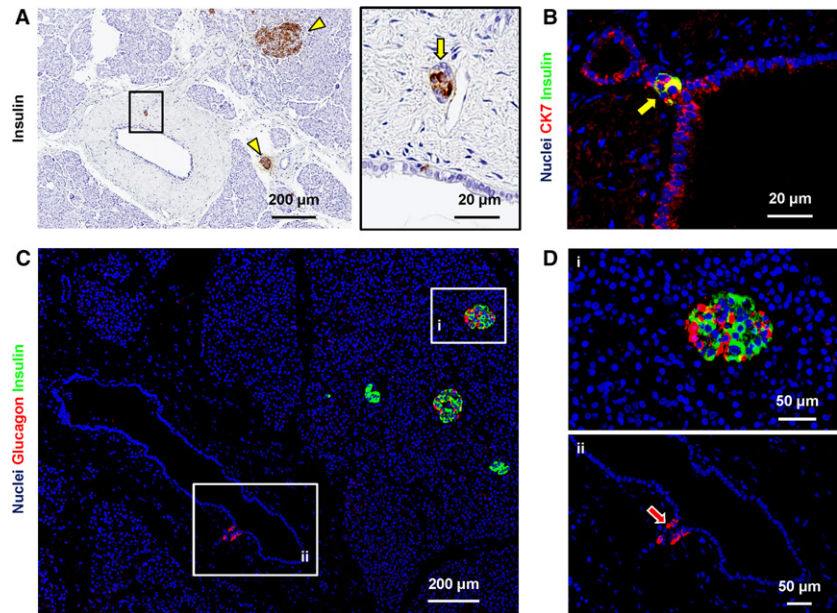
that the expression of these two pluripotency genes and other key stem cell markers (e.g. NANOG) shifted from nuclear to cytoplasmic or disappeared altogether with a shift from the PBGs in the hepato-pancreatic common duct to the neighbouring PDGs (Wang et al. 2013).

PDGs represent a unique compartment residing within the pancreatic duct wall. A previous paper by Thayer and associates showed that PDG intraductal pouches are more frequent in proximal ducts than peripheral ducts and that the distribution of these pouches is not uniform (Strobel et al. 2010). In the present manuscript, we further investigated the distribution of PDGs in the human pancreatic duct system on the basis of duct type and size. Our data indicate that PDGs are present in the main and larger interlobular pancreatic ducts. Interestingly, interlobular pancreatic ducts with a diameter < 300 μm do not display PDGs within their walls. Moreover, our results indicated that the PDGs consistently constituted nearly 4% of the wall of each duct examined. However, in agreement with the study of Thayer and associates (Strobel et al. 2010), the presence of PDGs correlated with the duct diameter. They were found to be more numerous in the main pancreatic duct at the head of the pancreas and progressively decreased with progression towards the tail and in larger interlobular ducts. Finally, they disappeared in interlobular ducts with a diameter < 300 μm.

From an anatomical point of view, PDGs represent the pancreatic counterparts of PBGs within the biliary tree. Both PDGs and PBGs are tubulo-alveolar glands composed of mucinous (acid and neutral mucins) and serous acini. The anatomical distribution of PDGs parallels that of PBGs within the intrahepatic biliary tree, where glands are only present in large bile ducts and their mass correlates with duct size (Carpino et al. 2012).

The study by Thayer and associates indicated that PDGs are composed mostly of mucin-producing cells (Strobel et al. 2010). However, our previous paper (Wang et al. 2013) and the present study provide further information regarding the progenitor cells within the human pancreatic duct system. In the present manuscript, we further characterized these niches and, in particular, showed that:

- PDGs represent novel anatomical niches of Sox9⁺ and Lgr5⁺ progenitor cells in the adult human pancreas.
- The cells in the PDG niches exhibit a pattern of phenotypic traits implying a radial maturational lineage axis of the progenitor cells.
- The proximal-to-distal maturational lineage axis starts with the PBGs in the hepato-pancreatic common duct, transitions to the main pancreatic duct and then to the interlobular pancreatic duct.

Our data indicate that PDGs represent a novel anatomical niche of [Oct4A⁻/Sox9⁺] and Lgr5⁺ cells in the adult human pancreas. In the development of the pancreas, the expression of Sox9 is essential for the maintenance of the pancreatic progenitor cell pool and has a key role in controlling the bi-potential (ductal and endocrine) progenitor cell population (Seymour et al. 2008; Furuyama et al. 2011; Seymour, 2014). Furthermore, in its commitment to the endocrine pancreas, Sox9 expression within the primitive epithelium is required for the induction of Ngn3, an indispensable gene for endocrine differentiation (Seymour et al. 2008; Shih et al. 2012; Seymour, 2014). Interestingly, Sox9⁺ PDG cells co-expressed Pdx1 but not Oct4A, indicating a committed progenitor rather than stem cell phenotype, an interpretation corroborating prior findings by us (Wang et al. 2013) and others (Zhou et al. 2007; Seifert & Xiong, 2014). A restricted Sox9⁺ sub-population also expressed
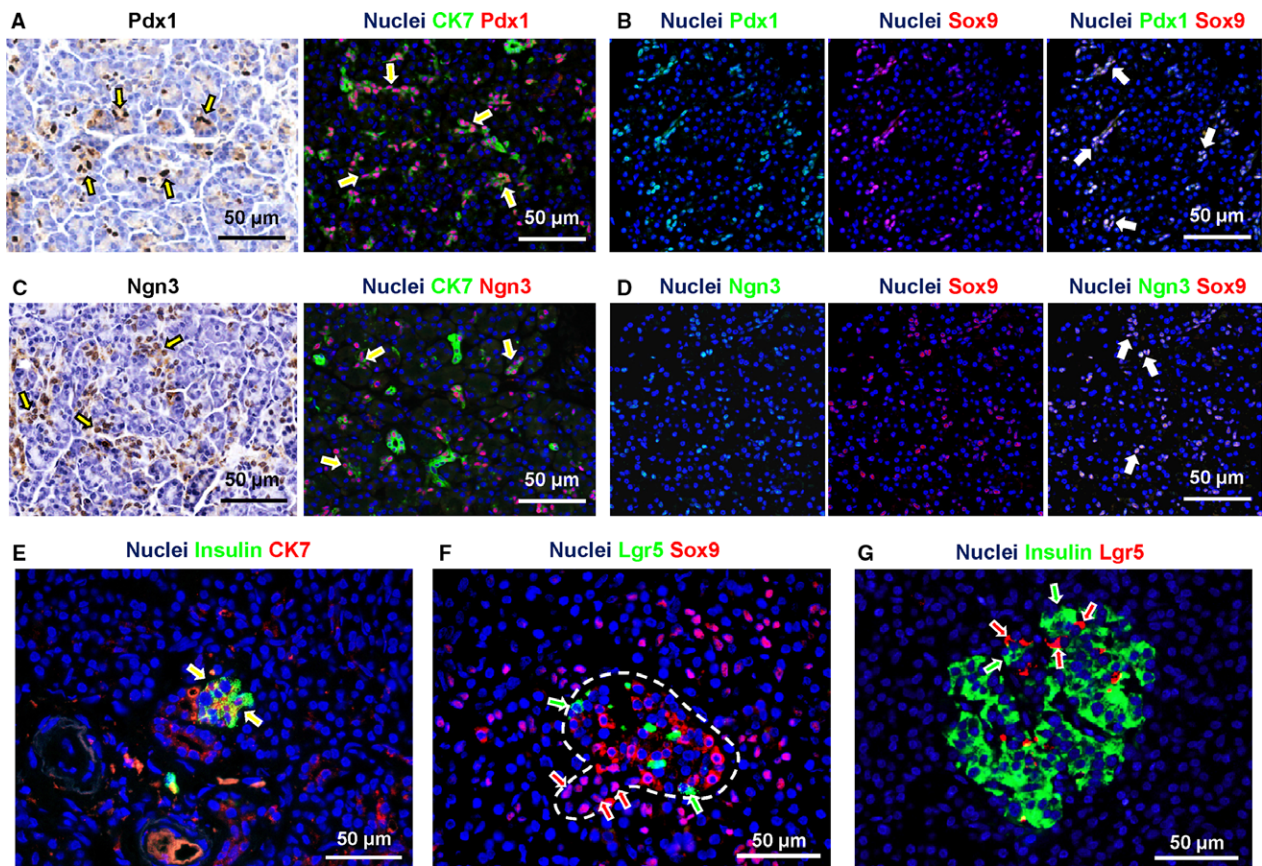
Fig. 6 Expression of progenitor cell markers in intercalated ducts. (A) Immunohistochemistry for Pdx1 and double immunofluorescence for Pdx1 and cytokeratin(CK)7. Intercalated ducts were diffusely Pdx1+ (arrows). (B) Double immunofluorescence for Pdx1 and Sox9 showed that Pdx1 mostly co-localized with Sox9 in intercalated duct cells (white nuclei in the merged image: arrows). (C) Immunohistochemistry for Ngn3 and double immunofluorescence for Ngn3 and CK7. Numerous intercalated duct cells were Ngn3+ (arrows). (D) Double immunofluorescence for Ngn3 and Sox9 showed that Ngn3 mostly co-localized with Sox9 in intercalated duct cells (white nuclei in the merged image: arrows). (E) Double immunofluorescence for insulin and CK7. Some intercalated ducts appeared in continuity with clusters of insulin+ cells organized in small pancreatic islet-like structures; in these cases, CK7+ duct cells were in direct continuity with islets. Moreover, CK7+/insulin+ cells were present at the interface between duct and islet (arrows). (F) Double immunofluorescence for Sox9 and Lgr5. Intercalated duct cells in continuity with endocrine islets had Sox9+ nuclei (red arrows); moreover, transitioning from duct to islet, cells lost nuclear Sox9 positivity. Lgr5+ cells were also present (two to three cells per islet) within pancreatic islets. Within the islets, Sox9 positivity did not overlap with Lgr5 expression (green arrows). (G) Double immunofluorescence for insulin and Lgr5; within the islets, Lgr5 positivity (red arrows) did not overlap with insulin expression (green arrows). In immunoflurescence images, nuclei are displayed in blue.

Ngn3, indicating features associated with the endocrine specification (Gomez et al. 2015). These observations indicate that PDGs represent the niche of a heterogeneous population of committed progenitor cells.

In the present manuscript, we investigated the expression of Lgr5 within adult human pancreata. Lgr5 is a marker in multiple organs of adult stem cells and progenitors of extensive proliferative potential (Clevers, 2013). In rodents, Lgr5 expression can be induced in regenerating pancreatic ducts by partial duct ligation (Huch et al. 2013; Dorrell et al. 2014). In these experimental conditions, Lgr5+ cells can be isolated from pancreatic ducts and cultured into pancreatic organoids; clonal pancreatic organoids can be induced to differentiate into duct as well as endocrine cells upon transplantation, thus proving their bi-potentiality (Huch et al. 2013). However, the fact that Oct4A was not expressed by

these Lgr5+ cells and that prior studies (Zhou et al. 2007; Wang et al. 2013; Seifert & Xiong, 2014) found no evidence of stem cells, implicate these as bipotent, committed progenitors. Our results indicate that Lgr5 is expressed in normal adult human pancreas, but its expression is limited to a restricted sub-population of Sox9+ and insulin/glucagon-negative progenitors found at the bottoms of PDGs within the duct walls. This sub-population could represent a more primitive cell compartment within the pancreas, potentially being intermediates (possibly transit amplifying cells?) that are highly proliferative.

Interestingly, Lgr5+ cells were found within pancreatic islets, but these cells were negative for Sox9 and endocrine markers. Thus, it is likely that Lgr5 expression implies the proliferative potential of the cells. Further studies are required to elucidate the relevance of Lgr5 expression.

Moreover, we showed that [Oct4A⁻/Sox9⁺/Pdx1⁺] cells, cells that are also PCNA⁺, were located primarily at the bottom of PDGs; by contrast, the cells at the surface epithelium were devoid of progenitor traits and were negative for PCNA. This suggests a radial-axis maturational lineage, paralleling that found within the biliary tree. The presumptive radial axis starts with early-stage proliferative progenitor cells at the bottom of PDGs, found deep within duct walls, and ends at the duct lumens with non-proliferative cells devoid of progenitor cell traits. These features support the concept that PDGs and their Sox9⁺ progenitor cell niches have a role in the renewal of the pancreatic duct epithelium (Yamaguchi et al. 2015).

Furthermore, we investigated the distribution within PDGs of key transcription factors implicated in the development of exocrine and endocrine pancreas. In our prior studies (Wang et al. 2013), we evaluated Pdx1 and Ngn3 expression in PDGs but without considering the location of the particular PDG within the pancreatic duct system. In the present manuscript, we evaluated the PDG phenotypic traits and correlated the traits with respect to their location. In particular, their distribution has been separately evaluated in PDGs associated with the main and interlobular pancreatic ducts. Interestingly, in the main pancreatic duct, the Sox9⁺ PDG cells were [Oct4A⁻/Pdx1⁺/Ngn3−]; interestingly, in the interlobular pancreatic ducts, Ngn-3⁺ PDG cells were more numerous than in the main pancreatic duct. Consistent with their potential to move towards an endocrine fate, a sub-population of PDG cells expressed pancreatic endocrine hormones such as insulin and glucagon. Insulin- (or glucagon) positive cells were more numerous in the interlobular duct than in the main pancreatic duct.

Our findings here complete our studies regarding the anatomical organization of niches of endodermal stem/progenitor cells and support the concept of a radial axis of a maturational lineage of stem cells and progenitors within the biliary tree and a parallel one of committed progenitors within the pancreas (Cardinale et al. 2011, 2012a; Carpino et al. 2012; Wang et al. 2013).

In adults, a proximal-to-distal maturational lineage axis is present starting with an abundance of stem cells in PBGs in the hepato-pancreatic common duct near to the duodenum, transitioning to committed progenitors and then to mature cells with progression along the biliary tree into the liver or into the pancreas (Cardinale et al. 2011, 2012a; Carpino et al. 2012; Wang et al. 2013). Here, we further demonstrated that, transitioning from the main pancreatic duct to the interlobular ducts, the PDGs modify their immunophenotype and reduce mucin production. A distinction between liver and pancreas is that cells retaining stem cell traits are present intrahepatically, whereas all cells within the pancreas are devoid of stem cell traits but retain properties indicative of committed progenitors (Zhou et al. 2007; Wang et al. 2013; Seifert & Xiong, 2014). The reason (s) for this distinction is not yet known.

Our results further indicate that the *in situ* PDG niche contains insulin- and glucagon-producing cells. However, the response of the PDG niche to hyperglycaemic conditions, and their role in generating insulin-producing cells in pathological conditions (e.g. diabetes) should be further evaluated.

In adult pancreas, another Sox9⁺ cell niche, besides that in the PDGs, is located throughout the epithelium of intercalated ducts, including the centro-acinar cells (Reichert & Rustgi, 2011; Kawaguchi, 2013). The potential of this niche to participate in the turnover of endocrine islets has been at the centre of a long-standing debate (Inada et al. 2008; Xu et al. 2008; Criscimanna et al. 2011; Furuyama et al. 2011; Kopp et al. 2011a,b; Hosokawa et al. 2015). Divergent studies have indicated the possibility that a subpopulation of Sox9⁺ cells can give rise to islet cells in the adult rodents, but this activation requires some form of injury (Criscimanna et al. 2011). In the present report, we demonstrated the expression of Pdx1 and Ngn3 by Sox9⁺ cells within human intercalated ducts. Our data on Sox9 expression in intercalated duct cells are consistent with the evidence in rodent pancreas (Seymour et al. 2007; Hosokawa et al. 2015) and human pancreas (Tanaka et al. 2013; Seymour, 2014). Actually, in the present study, the percentage of Sox9⁺ cells within intercalated ducts is slightly lower in comparison with that in the study of Tanaka et al. (2013). However, samples from Tanaka et al.'s study came from patients who underwent distal pancreatectomy for gastric cancer. In contrast, our samples were obtained from organs discarded during transplantation procedures, and we ruled out the presence of underlying biliary or pancreatic disorders. Therefore, the higher numbers of Sox9⁺ cells in the studies by Tanaka et al. (2013) could represent a cellular reaction to the pathological involvement of the pancreas which made the resection necessary.

Several lines of evidence in rodents have indicated that Pdx1 and Ngn3 are expressed in pancreatic ductal cells during embryological development but are restricted to islets in adult mice (Seymour et al. 2007; Wang et al. 2009; Seymour, 2014); however, in adult mouse pancreas, Ngn3 expression has been seen in ductal cells during islet regeneration after different types of injury (Xu et al. 2008; Collombat et al. 2009). Interestingly, our data in humans indicated that these transcription factors are expressed by intercalated duct cell in adults. Our observations are in accordance with other studies (Kobayashi et al. 2014; Gomez et al. 2015) and confirm the presence of endocrine features in ductal cells in adult human pancreas. Ductal Sox9⁺ cells are occasionally found in strict continuity with pancreatic islets, as reported elsewhere (Zhao et al. 2008). Moreover, cells with an intermediate phenotype (ductal/endocrine: CK7⁺/insulin⁺ can be found at the interface between ducts and islets. Furthermore, the progressive loss of Sox9 nuclear expression was observed moving from duct to islet. These observations suggest a transition from duct to islet and a

possible relationship between Sox9^{+} intercalated duct cells and pancreatic islet cells in adult humans. In general, our results seem to further underscore the heterogeneity between rodents and humans regarding spatial localization of pancreatic islets which is characterized by the prevalence of intralobularly located, peripheral duct islets in humans (Merkwitz et al. 2013).

In summary, a major point of this manuscript is the description in adult human pancreas of two distinct niches of Sox9^{+} (progenitor) cells with different immunophenotypes. Interestingly, no marker exists to precisely label and isolate putative progenitor cells within the pancreas. Therefore, a detailed immunophenotyping and a constellation of markers are necessary to characterize these cells and their anatomical location. In this context, our results indicated that Sox9^{+} cells are not restricted to intercalated or interlobular duct epithelium but are present also in PDGs; moreover, Sox9^{+}/Lgr5^{+} cells are restricted to PDGs, whereas duct epithelium is almost negative for Lgr5. Finally, Lgr5^{+} cells within pancreatic islets are Sox9^{−}.

Our results have important anatomic and patho-physiologic implications. The present manuscript clearly indicates the similarities between the pancreatic duct system and the intrahepatic biliary tree. Interestingly, both the pancreatic duct system and the intrahepatic and extrahepatic biliary tree are anatomically heterogeneous. The heterogeneity in the biliary tree also includes the physiological and proliferative capabilities of cholangiocytes lining larger or smaller ducts (Glaser et al. 2009) and has profound implications in biliary disorders (Carpino et al. 2015).

Also, the biliary tract and the pancreas are affected by a number of pathologies showing significant clinico-pathologic similarities; some of these pathologies affect the two organs simultaneously. Typical examples are:

- The IgG4-related disease that affects, in the same patient, the biliary tract, such as IgG4-related sclerosing cholangitis, and the pancreas, such as lympho-plasmatic sclerosing autoimmune pancreatitis (Okazaki et al. 2014).
- Pure mucin-secreting cholangiocarcinoma (CCA) showing extensive similarities with ductal pancreatic adenocarcinoma.
- Preneoplastic lesions of bile ducts and pancreatic ducts (Nakanuma et al. 2014).

Neoplastic diseases of bile ducts and pancreatic ducts merit further discussion. CCA and ductal pancreatic adenocarcinoma share similar pathologic features and genetic abnormalities (Nakanuma & Sato, 2014; Sato et al. 2014). PBGs have been proposed as the site of origin of CCA (Cardinale et al. 2012b; Igarashi et al. 2013), but our results also suggest that PDGs are candidate sites of origin of pancreatic intra-epithelial neoplasias (PanIN) and pancreatic duct adenocarcinomas. Also, in response to injury, PDGs undergo a mucinous metaplasia with PanIN features (Strobel et al.

2010). Furthermore, BrdU incorporation and production of pancreatic cancer-specific proteins in PDGs are increased in the course of experimental diabetes and chronic pancreatitis (Bobrowski et al. 2013). Moreover, the development of PanIN lesions *in vivo* may involve the emergence of a stem/progenitor-like population that expresses Sox9 and Pdx1 (Kopp et al. 2012; Delgiorno et al. 2014). Our results are consistent with this scenario. PDGs, in fact, contain Sox9^{+}/Pdx1^{+} progenitor cells and mucin-producing cells, and their anatomical distribution overlaps with sites at which pancreatic adenocarcinoma occurs.

Concluding remarks

The present manuscript further underscores the anatomical similarity between the biliary tree and pancreatic duct system. This link derives from a common embryologic origin and could have important implications in the patho-physiology of the biliary tract and the pancreas.

Acknowledgements

Conflict of interest

None to declare.

Author's contributions

G.C.: conception and design, acquisition and assembly of data, data analyses and interpretation; manuscript writing and editing. A.R.: acquisition and assembly of data, data analyses and interpretation, manuscript writing and editing. V.C. conception and design; data interpretation, manuscript editing. A.F., P.O., D.O.: acquisition and assembly of data, figure layout. P.B., M.R.: provision of study materials (specimens from liver transplantation). D.A. (senior author): manuscript editing, final approval of manuscript and financial support. L.R., E.G. (senior authors): conception and design, manuscript editing, final approval of manuscript and financial support.

References

Bobrowski A, Spitzner M, Bethge S, et al. (2013) Risk factors for pancreatic ductal adenocarcinoma specifically stimulate pancreatic duct glands in mice. *Am J Pathol* **182**, 965–974.

Burke ZD, Tosh D (2012) Ontogenesis of hepatic and pancreatic stem cells. *Stem Cell Rev* **8**, 586–596.

Cardinale V, Wang Y, Carpino G, et al. (2011) Multipotent stem/progenitor cells in human biliary tree give rise to hepatocytes, cholangiocytes, and pancreatic islets. *Hepatology* **54**, 2159–2172.

Cardinale V, Wang Y, Carpino G, et al. (2012a) The biliary tree – a reservoir of multipotent stem cells. *Nat Rev Gastroenterol Hepatol* **9**, 231–240.

Cardinale V, Wang Y, Carpino G, et al. (2012b) Mucin-producing cholangiocarcinoma might derive from biliary tree stem/progenitor cells located in peribiliary glands. *Hepatology* **55**, 2041–2042.

Carpino G, Cardinale V, Onori P, et al. (2012) Biliary tree stem/progenitor cells in glands of extrahepatic and intraheptic bile ducts: an anatomical in situ study yielding evidence of maturational lineages. *J Anat* **220**, 186–199.

Carpino G, Cardinale V, Gentile R, et al. (2014) Evidence for multipotent endodermal stem/progenitor cell populations in human gallbladder. *J Hepatol* **60**, 1194–1202.

Carpino G, Cardinale V, Renzi A, et al. (2015) Activation of biliary tree stem cells within peribiliary glands in primary sclerosing cholangitis. *J Hepatol* **63**, 1220–1228.

Clevers H (2013) The intestinal crypt, a prototype stem cell compartment. *Cell* **154**, 274–284.

Collombat P, Xu X, Ravassard P, et al. (2009) The ectopic expression of Pax4 in the mouse pancreas converts progenitor cells into alpha and subsequently beta cells. *Cell* **138**, 449–462.

Criscimanna A, Speicher JA, Houshmand G, et al. (2011) Duct cells contribute to regeneration of endocrine and acinar cells following pancreatic damage in adult mice. *Gastroenterology* **141**, 1451–1462.e1–6.

Delgiorno KE, Hall JC, Takeuchi KK, et al. (2014) Identification and manipulation of biliary metaplasia in pancreatic tumors. *Gastroenterology* **146**, 233–244.e5.

Dorrell C, Tarlow B, Wang Y, et al. (2014) The organoid-initiating cells in mouse pancreas and liver are phenotypically and functionally similar. *Stem Cell Res* **13**, 275–283.

Furuyama K, Kawaguchi Y, Akiyama H, et al. (2011) Continuous cell supply from a Sox9-expressing progenitor zone in adult liver, exocrine pancreas and intestine. *Nat Genet* **43**, 34–41.

Glaser SS, Gaudio E, Rao A, et al. (2009) Morphological and functional heterogeneity of the mouse intrahepatic biliary epithelium. *Lab Invest* **89**, 456–469.

Gomez DL, O'Driscoll M, Sheets TP, et al. (2015) Neurogenin 3 expressing cells in the human exocrine pancreas have the capacity for endocrine cell fate. *PLoS One* **10**, e0133862.

Hosokawa S, Furuyama K, Horiguchi M, et al. (2015) Impact of Sox9 dosage and Hes1-mediated Notch signaling in controlling the plasticity of adult pancreatic duct cells in mice. *Sci Rep* **5**, 8518.

Huch M, Bonfanti P, Boj SF, et al. (2013) Unlimited *in vitro* expansion of adult bi-potent pancreas progenitors through the Lgr5/R-spondin axis. *EMBO J* **32**, 2708–2721.

Igarashi S, Sato Y, Ren XS, et al. (2013) Participation of peribiliary glands in biliary tract patho-physiologies. *World J Hepatol* **5**, 425–432.

Inada A, Nienaber C, Katsuta H, et al. (2008) Carbonic anhydrase II-positive pancreatic cells are progenitors for both endocrine and exocrine pancreas after birth. *Proc Natl Acad Sci U S A* **105**, 19915–19919.

Kawaguchi Y (2013) Sox9 and programming of liver and pancreatic progenitors. *J Clin Invest* **123**, 1881–1886.

Kobayashi M, Fujinaga Y, Ota H (2014) Reappraisal of the immunophenotype of pancreatic intraductal papillary mucinous neoplasms (IPMNs) – gastric pyloric and small intestinal immunophenotype expression in gastric and intestinal type IPMNs. *Acta Histochem Cytochem* **47**, 45–57.

Kopp JL, Dubois CL, Hao E, et al. (2011a) Progenitor cell domains in the developing and adult pancreas. *Cell Cycle* **10**, 1921–1927.

Kopp JL, Dubois CL, Schaffer AE, et al. (2011b) Sox9+ ductal cells are multipotent progenitors throughout development but do not produce new endocrine cells in the normal or injured adult pancreas. *Development* **138**, 653–665.

Kopp JL, von Figura G, Mayes E, et al. (2012) Identification of Sox9-dependent acinar-to-ductal reprogramming as the principal mechanism for initiation of pancreatic ductal adenocarcinoma. *Cancer Cell* **22**, 737–750.

Liu H, Yang H, Zhu D, et al. (2014) Systematically labeling developmental stage-specific genes for the study of pancreatic beta-cell differentiation from human embryonic stem cells. *Cell Res* **24**, 1181–1200.

Lysy PA, Weir GC, Bonner-Weir S (2012) Concise review: pancreas regeneration: recent advances and perspectives. *Stem Cells Transl Med* **1**, 150–159.

Merkwitz C, Blaschuk OW, Schulz A, et al. (2013) The ductal origin of structural and functional heterogeneity between pancreatic islets. *Prog Histochem Cytochem* **48**, 103–140.

Nakanuma Y (2010) A novel approach to biliary tract pathology based on similarities to pancreatic counterparts: is the biliary tract an incomplete pancreas? *Pathol Int* **60**, 419–429.

Nakanuma Y, Sato Y (2014) Hilar cholangiocarcinoma is pathologically similar to pancreatic duct adenocarcinoma: suggestions of similar background and development. *J Hepatobiliary Pancreat Sci* **21**, 441–447.

Nakanuma Y, Harada K, Sasaki M, et al. (2014) Proposal of a new disease concept 'biliary diseases with pancreatic counterparts'. Anatomical and pathological bases. *Histol Histopathol* **29**, 1–10.

Nobili V, Carpino G, Alisi A, et al. (2012) Hepatic progenitor cells activation, fibrosis and adipokines production in pediatric nonalcoholic fatty liver disease. *Hepatology* **56**, 2142–2153.

Nobili V, Carpino G, Alisi A, et al. (2014) Role of docosahexaenoic acid treatment in improving liver histology in pediatric nonalcoholic fatty liver disease. *PLoS One* **9**, e88005.

Okazaki K, Yanagawa M, Mitsuyama T, et al. (2014) Recent advances in the concept and pathogenesis of IgG4-related disease in the hepato-bilio-pancreatic system. *Gut Liv* **8**, 462–470.

Razavi R, Najafabadi HS, Abdullah S, et al. (2015) Diabetes enhances the proliferation of adult pancreatic multipotent progenitor cells and biases their differentiation to more beta-cell production. *Diabetes* **64**, 1311–1323.

Reichert M, Rustgi AK (2011) Pancreatic ductal cells in development, regeneration, and neoplasia. *J Clin Invest* **121**, 4572–4578.

Sato Y, Harada K, Sasaki M, et al. (2014) Cystic and micropapillary epithelial changes of peribiliary glands might represent a precursor lesion of biliary epithelial neoplasms. *Virchows Arch* **464**, 157–163.

Seifert BA, Xiong Y (2014) Out of the F-box: reawakening the pancreas. *Cell Stem Cell* **15**, 111–112.

Semeraro R, Carpino G, Cardinale V, et al. (2012) Multipotent stem/progenitor cells in the human foetal biliary tree. *J Hepatol* **57**, 987–994.

Seymour PA (2014) Sox9: a master regulator of the pancreatic program. *Rev Diabet Stud* **11**, 51–83.

Seymour PA, Freude KK, Tran MN, et al. (2007) SOX9 is required for maintenance of the pancreatic progenitor cell pool. *Proc Natl Acad Sci U S A* **104**, 1865–1870.

Seymour PA, Freude KK, Dubois CL, et al. (2008) A dosage-dependent requirement for Sox9 in pancreatic endocrine cell formation. *Dev Biol* **323**, 19–30.

Shih HP, Kopp JL, Sandhu M, et al. (2012) A Notch-dependent molecular circuitry initiates pancreatic endocrine and ductal cell differentiation. *Development* **139**, 2488–2499.

Smukler SR, Arntfield ME, Razavi R, et al. (2011) The adult mouse and human pancreas contain rare multipotent stem cells that express insulin. *Cell Stem Cell* **8**, 281–293.

Strobel O, Rosow DE, Rakhlin EY, et al. (2010) Pancreatic duct glands are distinct ductal compartments that react to chronic injury and mediate Shh-induced metaplasia. *Gastroenterology* **138**, 1166–1177.

Tanaka T, Kuroki T, Adachi T, et al. (2013) Evaluation of SOX9 expression in pancreatic ductal adenocarcinoma and intraductal papillary mucinous neoplasm. *Pancreas* **42**, 488–493.

Udager A, Prakash A, Gumucio DL (2010) Dividing the tubular gut: generation of organ boundaries at the pylorus. *Prog Mol Biol Transl Sci* **96**, 35–62.

Wandzioch E, Zaret KS (2009) Dynamic signaling network for the specification of embryonic pancreas and liver progenitors. *Science* **324**, 1707–1710.

Wang S, Jensen JN, Seymour PA, et al. (2009) Sustained Neurog3 expression in hormone-expressing islet cells is required for endocrine maturation and function. *Proc Natl Acad Sci U S A* **106**, 9715–9720.

Wang Y, Lanzoni G, Carpino G, et al. (2013) Biliary tree stem cells, precursors to pancreatic committed progenitors: evidence for possible life-long pancreatic organogenesis. *Stem Cells* **31**, 1966–1979.

Xu X, D'Hoker J, Stange G, et al. (2008) Beta cells can be generated from endogenous progenitors in injured adult mouse pancreas. *Cell* **132**, 197–207.

Yamaguchi J, Liss AS, Sontheimer A, et al. (2015) Pancreatic duct glands (PDGs) are a progenitor compartment responsible for pancreatic ductal epithelial repair. *Stem Cell Res* **15**, 190–202.

Zhao HL, Sui Y, Guan J, et al. (2008) Topographical associations between islet endocrine cells and duct epithelial cells in the adult human pancreas. *Clin Endocrinol (Oxf)* **69**, 400–406.

Zhou Q, Law AC, Rajagopal J, et al. (2007) A multipotent progenitor domain guides pancreatic organogenesis. *Dev Cell* **13**, 103–114.

Supporting Information

Additional Supporting Information may be found in the online version of this article:

Fig. S1. Control for labelling two primary rabbit antibodies.

Fig. S2. Controls for IHC and IF staining for Ngn3.

Fig. S3. High magnification of Fig. 6D showing that Ngn3 positivity does not entirely correspond to Sox9 positivity in double immunoflurescence stains.